The Plasma-Induced Leukemia Cell Death is Dictated by the ROS Chemistry and the HO-1/CXCL8 Axis

Sander Bekeschus, Ramona Clemen, Lyubomir Haralambiev, Felix Niessner, Piotr Grabarczyk, Klaus-Dieter Weltmann, *Member, IEEE*, Jonas Menz, Matthias Stope, Thomas von Woedtke, Rajesh Gandhirajan, and Anke Schmidt

***Abstract*—Cold physical plasma-derived reactive oxygen specie (ROS) inactivate cells, which might be beneficial in oncology. However, several aspects of plasma oncotherapy remain elusive. These include the identification of an ROS composition with maximum toxicity and the molecular mechanisms that govern the degree of plasma-induced cell death. Using two human leukemia cell lines and the plasma jet kINPen, we identified Jurkat cells to be most sensitive to argon plasma while THP-1 cells were most sensitive to He/O_2 plasma. Screening of 20 protein transcripts involved in redox regulation identified HMOX1 as a commonly regulated element, and siRNA-mediated knockdown of the HMOX1-transcribed protein HO-1 augmented plasma-derived cell death in the two leukemia cell lines. Interestingly, knockdown of the H_2O_2-decomposing enzyme catalase did not elevate plasma-induced cell death. By contrast, siRNA-mediated suppression of the production of the chemokine CXCL8 (IL8) markedly enhanced plasma-derived cytotoxicity up to twofold. *Vice versa*, by antibody-mediated blocking of IL8 receptors, a massive increase in IL8 and HO-1 secretion was observed, together with a dramatically enhanced cell death in response to plasma treatment, especially in THP-1 cells. These results suggest that the plasma-induced leukemia cell death is dictated by the ROS chemistry and the HO-1/CXCL8 axis via paracrine or autocrine IL8-mediated pro-survival signaling.**

***Index Terms*—HMOX1, IL8, Jurkat, kINPen, oncology, plasma medicine, THP-1.**

Manuscript received June 29, 2020; revised August 24, 2020; accepted August 28, 2020. Date of publication September 2, 2020; date of current version May 3, 2021. This work was supported in part by the German Federal Ministry of Education and Research (BMBF) under Grant 03Z22DN11 and Grant 03Z22Di1; and in part by the European Social Fund and the Ministry of Education, Science, and Culture of Mecklenburg-Vorpommern under Grant ESF/14-BM-A55-0006-18. *(Corresponding author: Sander Bekeschus.)*

Sander Bekeschus, Felix Niessner, Klaus-Dieter Weltmann, Rajesh Gandhirajan, and Anke Schmidt are with the ZIK Plasmatis, Leibniz Institute for Plasma Science and Technology (INP), 17489 Greifswald, Germany (e-mail: sander.bekeschus@inp-greifswald.de).

Ramona Clemen is with the ZIK plasmatis, Leibniz Institute for Plasma Science and Technology (INP), 17489 Greifswald, Germany, and also with the Department of Immunology, Greifswald University Medical Center, 17475 Greifswald, Germany.

Lyubomir Haralambiev is with the Department of Trauma, Reconstructive Surgery and Rehabilitation Medicine, Greifswald University Medical Center, 17475 Greifswald, Germany, and also with the Department of Trauma and Orthopaedic Surgery, BG Emergency Hospital Berlin, 12683 Berlin, Germany.

Piotr Grabarczyk is with the Institute of Hematology and Oncology, Greifswald University Medical Center, 17475 Greifswald, Germany.

Jonas Menz is with the ZIK Plasmatis, Leibniz Institute for Plasma Science and Technology (INP), 17489 Greifswald, Germany, and also with the Department of General, Visceral, Thoracic and Vascular Surgery, Greifswald University Medical Center, 17475 Greifswald, Germany.

Matthias Stope is with the Department of Gynecology and Gynecological Oncology, University Hospital Bonn, 53127 Bonn, Germany.

Thomas von Woedtke is with the ZIK Plasmatis, Leibniz Institute for Plasma Science and Technology (INP), 17489 Greifswald, Germany, and also with the Institute for Hygiene and Environmental Medicine, Greifswald University Medical Center, 17489 Greifswald, Germany.

Color versions of one or more figures in this article are available at https://doi.org/10.1109/TRPMS.2020.3020686.

Digital Object Identifier 10.1109/TRPMS.2020.3020686

I. Introduction

COLD physical plasma is a partially ionized gas that is currently used as an accredited medical procedure to support wound healing in Europe [1]. Besides its documented antimicrobial and stimulating effects in skin cells [2], [3], emerging evidence in the last decade also pointed to a potent tumor-toxicity with extended plasma treatment [4], [5]. To date, plasma exposure was shown to inactivate cancer cells of various origins, including the pancreas [6]–[8], leukemia [9]–[11], breast [12]–[14], ovarian [15]–[17], colon [18]–[20], skin [21]–[23], head and neck [24]–[26], and the brain [27]–[29]. First patients suffering from stage IV head and neck squamous cell carcinoma have benefited from plasma therapy in a palliative setting [30]–[32].

Many preclinical studies and first clinical evidence appear promising, but the molecular basis of plasma-mediated tumor toxicity is less clear. It is understood that the primary mechanism of action by which gas plasmas target cells and tissues is the loco-regional deposition of a plethora of reactive oxygen species (ROSs) generated during plasma treatment [33]. Currently, the holy grail of plasma medicine is the identification of the optimal ROS mixture that maximizes tumor-toxic effects. While plasma systems using the ambient air, such as many dielectric barrier discharges, can be controlled mostly by their electrical parameters, the majority of plasma jets utilize noble gases, such as helium and argon [34]. Such plasma jets can be modulated elegantly by admixing molecular gases, such as O_2 and N_2. This way, the ROS composition can be shifted toward control of, for instance, nitric oxide, atomic oxygen, and hydroxyl radical production [35], [36]. While many studies, including our own, have successfully attempted to optimize the feed gas for maximum toxicity [37]–[41],

evidence on its broad applicability across several cell lines is scarce. Along similar lines, several reports noted differences in the sensitivity of different cancer lines toward plasma treatment, but the underlying molecular mechanisms related to plasma-derived ROS and its cell death induction remain largely elusive.

To decipher both optimal plasma-derived ROS compositions as well as cellular proteins dictating the sensitivity of cells to the plasma-induced cell death, we utilized an atmospheric pressure plasma jet and two human leukemia cell lines Jurkat and THP-1 to tackle these challenges. Similar to their primary counterparts [42], these cell types differ in their sensitivity to plasma at a maximum degree [43], [44], allowing conclusions their sensitivity to plasma treatment in the presence or absence of target proteins. The intention was to use both cell types for a proof-of-concept study that can be extended for further cell types and plasma sources, rather than claiming a therapeutic benefit. It was found that both cell lines showed maximum sensitivity, not to a similar but different feed gas composition and that the siRNA-mediated knockdown of the proteins heme oxygenase 1 (HO-1) and interleukin 8 (IL8, also known as chemokine CXCL8) as well as receptor-blockage of the IL8-receptors (IL8R, also known as CXCR1 and CXCR2) vastly enhanced plasma-induced cytotoxicity.

II. Methods

A. Cell Culture

The human leukemia lymphocyte cell line Jurkat (ATCC TIB-152) and monocyte cell line THP-1 (ATCC TIB-202), as well as the human melanoma cell line SK-MEL-28 (SKM; ATCC HTB-72), were cultured in Roswell Park Memorial Institute (RPMI) 1640 cell culture medium supplemented with 10% fetal bovine serum, 1% penicillin/streptomycin, and 1% glutamine (all Sigma, Germany) under standard cell culture conditions (37 °C, 5% CO_2, 95% humidity). Cells were subcultured two to three times per week.

B. Plasma Jet and Treatment of Cells

The atmospheric pressure plasma jet kINPen (neoplas tools, Germany) was utilized. It is similar in construction to the clinically accredited kINPen MED and was operated at 1 MHz. The plasma jet was attached to a software-controlled, motorized *xyz*-table (CNC step, Germany) capable of hovering over the center of each well at a predefined jet-to-well distance with 10-μm precision. Feed gas modulation was performed using an eight-channel flow controller unit (MKS, Germany) that was factor-adjusted to each of the gases used in this study (argon, helium, oxygen, nitrogen; all >99.99% purity; Air Liquide, Germany). For treatment, 1×10^5 viable cells in 400 μl of fully supplemented cell culture medium were added to 24-well plates and treated with each of the plasma gas conditions for either 10 s (Jurkats) or 30 s (THP-1). Viable-cell-determinations were performed with high accuracy using acoustic focusing flow cytometry (attune nxt; Applied Biosystems, USA) with dead cell exclusion via propidium iodide (PI). Feed gas addition was 1% for oxygen and nitrogen with a bulk gas flux of argon and helium of 0.5 to 2.0 standard liters per minute (slm). At 4 h, the cells were subjected to metabolic activity analysis or pelleted and stored at −20 °C for gene expression analysis. For transfection experiments, only argon plasma treatment was performed at 2.0 slm, and cells were analyzed 24 h later.

C. Metabolic Activity, Cell Viability, and Flow Cytometry

The cells were incubated for 2 h with resazurin (100 μM; Alfa Aesar, USA) to determine the metabolic activity. During incubation at 37 °C, metabolically active cells reduce resazurin to its fluorescent form, resorufin. The fluorescence was quantified using a multimode fluorescence plate reader at λ_{ex} 535 nm and λ_{em} 590 nm (Tecan, Switzerland), and fluorescence intensities of samples were normalized against those of untreated cells for each cell line separately. For live-cell imaging experiments, the cells were incubated with CellEvent caspase 3/7 detection reagent (Thermo, USA) to identify apoptosis, and 4',6-diamidino-2-phenylindole (DAPI; BioLegend, USA) to identify terminally dead cells. Cells were imaged at 6 h post plasma treatment using a high content imaging device (Operetta CLS; PerkinElmer, Germany) with a 20× (NA: 0.4) air objective (Zeiss, Germany) using the bright-field channel, the λ_{ex} 475 nm λ_{em} 525±25 nm channel to detect fluorescence of the caspase 3/7 activation, and the λ_{ex} 405 nm λ_{em} 465±35 nm channel to detect DAPI fluorescence when bound to DNA. *Harmony* 4.9 (PerkinElmer, Germany) served as image analysis software. DAPI was also used to identify the relative distribution of cells with compromised cell membranes using flow cytometry (CytoFLEX S; Beckman-Coulter, USA). The relative expression intensities of CD181 (CXCR1) and CD182 (CXCR2) were analyzed using flow cytometry. 24 h after plasma treatment, cells were harvested, washed with phosphate-buffered saline (PBS), and incubated with monoclonal antibodies conjugated with fluorochromes (anti-CD181-phycoerythrin and anti-CD182 allophycocyanin; both BioLegend, U.K.), before analyzing the mean fluorescence intensity (MFI) of each antibody in the viable ($DAPI^-$) cell fraction. In a second setting, the cells were preincubated with the antibody or recombinant human interleukin (IL) 8 (100 ng/ml; BioLegend, U.K.), followed by plasma treatment and cell viability analysis using flow cytometry 24-h later. *Kaluza* 2.1.1 (Beckman-Coulter, USA) served as flow cytometry analysis software.

D. mRNA Quantification

After 4 h of incubation of the untreated or plasma-treated cells, cells were taken off or scratched off the dishes and transferred into 1.5 ml tubes (Eppendorf, Germany). After pelleting and suspending in lysis buffer, RNA isolation was performed according to the manufacturer's protocol (RNA Mini Kit; Bio&SELL, Germany). The RNA concentration of each sample was measured by using the NanoDrop 2000C (Thermo, USA) device. The RNA was aliquoted into micro-tubes for further experiments. For quantitative polymerase chain reaction (qPCR), 1 μg of RNA was synthesized into cDNA according to the manufacturer's instructions (ThermoFisher, USA)

using a thermocycler (Biometra, Germany). qPCR was performed in white 96-well V-bottom plates with Sybr Green (BioRad, Germany) labeled targets over 40-cycles using a Light Cycler 480 machine (Roche, Switzerland). Fold changes in expression in relation to the house-keeping gene GAPDH were calculated using the $2^{-\Delta\Delta Ct}$ method.

E. siRNA-Mediated Knockdown and Protein Validation

The cells were transfected with different siRNAs using an Amaxa electroporation device in combination with the Cell Line Nucleofector Kit V (Lonza, Germany). For this, 1×10^6 cells (per condition) were suspended in 100 μl of the transfection buffer from the kit. Transfection was performed either in the absence (mock) or presence of nontargeting control (NTC: luciferase) or targeting (HMOX1, catalase, IL8) siRNA (Thermo, USA). The catalog numbers of the ESI siRNAs are EHU051241 (HMOX1), EHU048671 (catalase), and EHU048321 (IL8). Three hundred nanograms of the respective siRNA were added to the cells to be transfected using special electroporation cuvettes. After electroporation, the cell suspension was transferred to the cell culture medium and rested for 24 h at 37 °C. Western blot was performed to validate protein knockdown. For this, transfected cells were pelleted, washed, lysed, and degraded in 100 μl of NuPAGE LDS Sample Buffer (Thermo, USA) and Dithiothreitol (1× LDS + 10% DTT) for 5 min at 96 °C. 40 microliters of each sample were transferred to gels (Thermo, USA) for the separation of proteins by their mass using electrophoresis. The proteins were blotted on a membrane, which was then transferred to *Roti-Block-Solution* (Carl Roth, Germany) containing the primary murine antibodies targeting β-actin, and one of the target proteins (catalase, HO-1, or IL8; all SantaCruz, USA). After washing, labeling with secondary antibodies (anti-mouse antibody conjugated to horseradish peroxide, HRP; SantaCruz, USA) was performed. Signal detection was done using 5-amino-2,3-dihydro-1,4-phthalazine dione (luminol) enhancer and stable peroxide SuperSignal (both ThermoFisher, USA). HRP-mediated catalysis of luminol to its oxidized form was quantified by detecting the luminescence emitted in this reaction (ImageQuant LAS 4000; GE Healthcare, Switzerland). For the analysis of IL8 and HO-1 in cell culture supernatants 24 h after plasma treatment, commercially available IL8 and HO-1 ELISAs were used according to the manufacturer's instructions (IL8: BioLegend, U.K.; HO-1: Abcam; U.K.), and absolute concentrations were obtained against a known standard.

F. Statistical Analysis

Statistical analysis was done using prism 8.4 (GraphPad Software, USA), using *t*-test or analysis of variances.

III. Results

A. Jurkat Cells Were Most Sensitive to Argon Plasma While THP-1 Cells Were Most Sensitive to He/O_2 Plasma

Modulating the feed gas composition of plasma jets changes their reactive species output in terms of composition and concentration. Details on the specific ROS and RNS output concerning the different feed gas compositions used were outlined previously [35], [37], [41], [45]–[54]. To identify the most cytotoxic feed gas composition in human leukemia cells, plasma treatment was performed [Fig. 1(a)], and the metabolic activity was assessed 4 h after treatment [Fig. 1(b)]. At 2 slm, argon plasma treatment showed the highest toxicity in Jurkat cells with significant differences when compared to all of the other gas conditions employed in this study [Fig. 1(c)]. By contrast, the He/O_2 conditions at 2 slm gave the most substantial decrease in the THP-1 cells' metabolic activity [Fig. 1(d)]. At lower feed gas fluxes of 0.5 slm and 1.0 slm, similar tendencies were observed in both cell lines, although not all comparisons reached statistical significance. This result is remarkable because it shows one cell line being most sensitive to one plasma-derived ROS composition, while a second cell line showed the sharpest decline in metabolic activity to another, chemically less related ROS composition. This is interesting also because the cell lines were both of leukemic origin. To further test the mode of cell death, cells were stained for the apoptosis marker of activated caspases 3 and 7. In Jurkat cells, apoptosis was induced at a high degree while that of THP-1 cells was less pronounced at 6 h following plasma treatment [Fig. 1(e)]. As we wanted to identify the molecular basis of plasma-induced changes in subsequent experiments, we added another cell line to our experiments. The SK-MEL-28 (SKM) melanoma cells were also sensitive to argon plasma [Fig. 1(f)] and He/O_2 plasma treatment [Fig. 1(g)], and the decrease in metabolic activity was overall similar to that of THP-1 but not Jurkat cells.

B. HMOX1 Was Commonly Upregulated in Three Plasma-Treated Cancer Cell Lines

Plasmas generate a plethora of ROS that are not only cytotoxic but also have signaling functions. Hence, it seemed plausible to screen the expression of redox-related proteins that, in principle, may be engaged by intracellular changes in the redox environment. To this end, we first performed a baseline expression of transcripts of 20 redox-related proteins in Jurkat, SKM, and THP-1 cells [Fig. 2(a)]. Their functions were previously described [55]. For protein disulfide isomerase family A member 2 (PDIA2), nucleoredoxin (NXN), glutaredoxin 1 (GLRX1), and GLRX3, the expression was either absent, below the detection limit, or not detected because of the primers not binding properly to the target transcripts. Additionally, SKM cells were void of peroxiredoxin 2 (PRDX2) mRNA, suggesting either a mutated sequence or an absence of PRDX2 in these cells. To condense the data further, relative expression intensities were normalized to that of the most sensitive cell line in our study, Jurkat cells [Fig. 2(b)]. Statistical analysis identified many significant differences at ±2-fold change levels. The THP-1 cells had significantly higher levels of the oxidoreductase and chaperone P4HB. In comparison, SKM cells had significantly higher levels in thioredoxin reductase 1 (TNXRD1) protecting from oxidative stress, NAD(P)H dehydrogenase quinone 1 (NQO1) regulating ubiquitin-independent p53 degradation and preventing

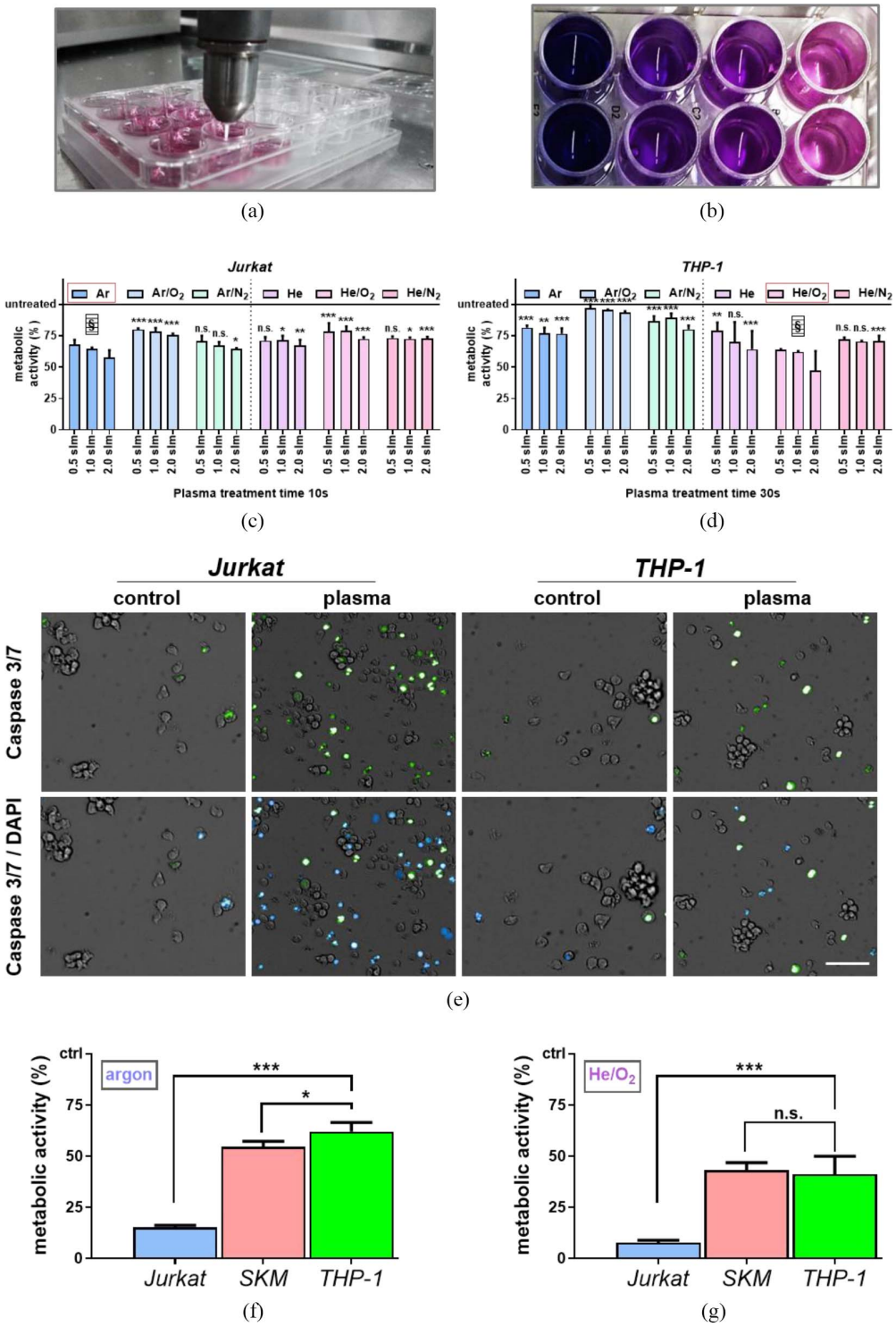

Fig. 1. Optimal cytotoxic feed gas composition differed depending on the cell type investigated. (a) Image of the plasma treatment setup. (b) Representative image of the resazurin assay used to investigate the metabolic activity that correlates with the pink color of the transformed resorufin. (c) and (d) Metabolic activity of Jurkat cells (c) and THP-1 cells (d) 4 h after exposure to plasma with different feed gas combinations and fluxes (0.5–2.0 slm) for 10 s and 30 s for each cell type, respectively. (e) Representative fluorescence microscopy images indicative of apoptosis (green) and terminal cell death (blue) in both Jurkat and THP-1 cells at 6 h after plasma treatment of one experiment. (f) and (g) Metabolic activity of Jurkat, SKM, and THP-1 cells 24 h after argon (f) or He/O_2 (g) plasma treatment for 20 s and 40 s, respectively. Data represent mean and S.E. of three independent experiments; statistical analysis was performed using two-way analysis of variances with Dunnett posthoc testing against argon (c) or He/O_2 (d), or one-way analysis of variances (f) and (g); * = $p < 0.05$, ** = $p < 0.01$, *** = $p < 0.001$; the scale bar is 100 μm; n.s. = not significant, slm = slm, Ar = argon, He = helium, SKM = SK-MEL-28; § indicates the most toxic feed gas composition for each Jurkat and THP-1 cells, respectively.

oxidative stress, and heme oxygenase 1 (HMOX1) important in heme catabolism and generating anti-inflammatory carbon monoxide. To identify the regulatory role of plasma treatment in the expression of the 20 redox-regulated genes, the three cell types were exposed to either argon or He/O_2 plasma. At 4 h, gene expression was identified using qPCR screening, and

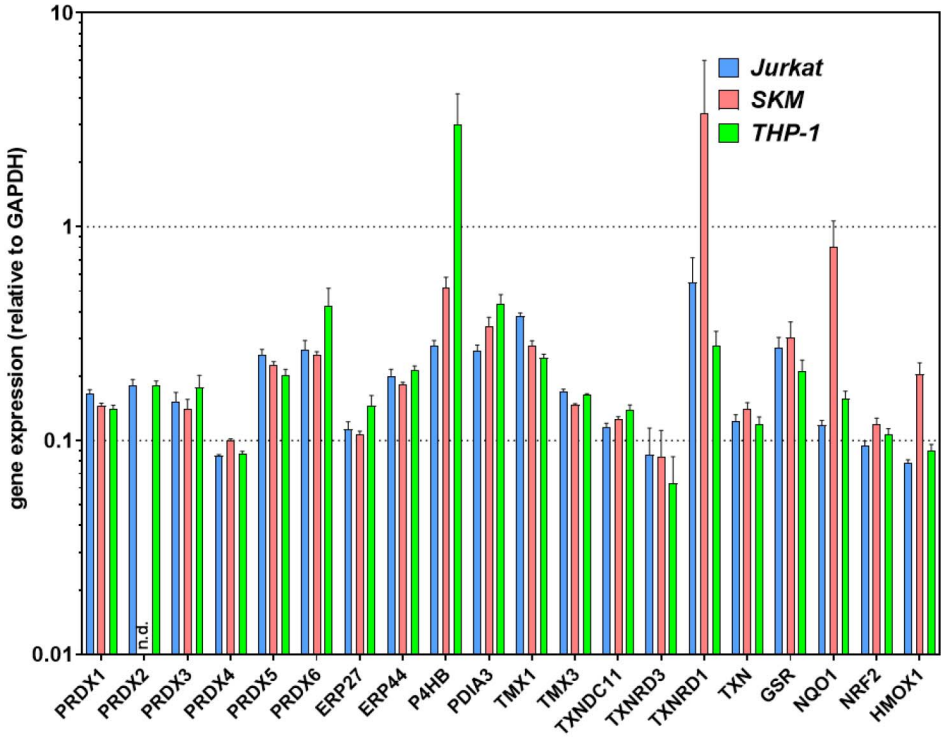

(a)

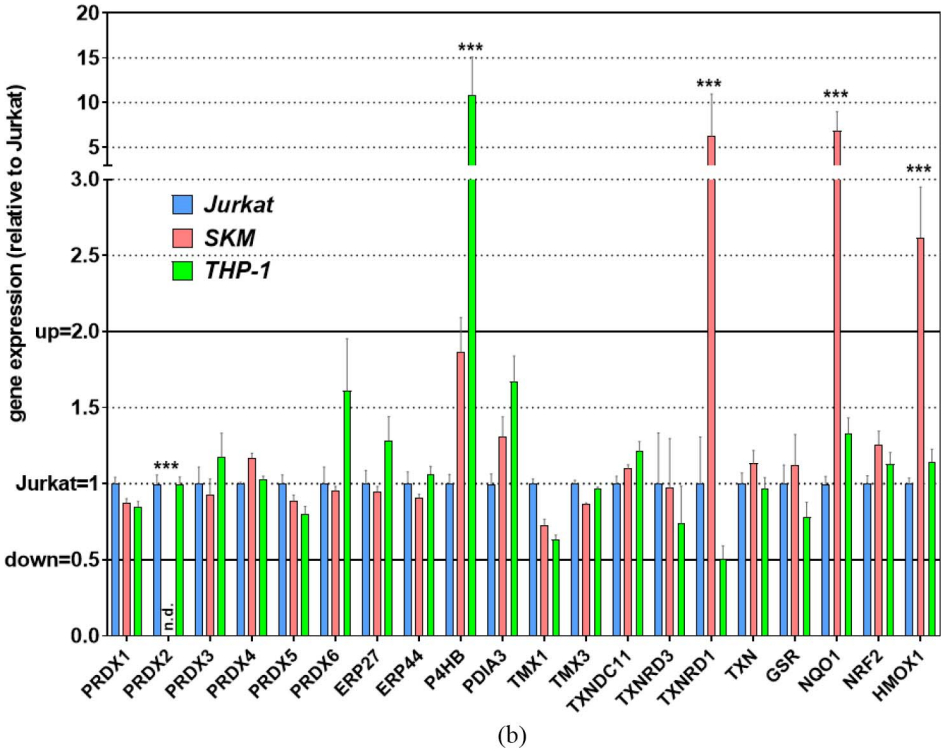

(b)

Fig. 2. Baseline mRNA expression of 20 redox-related target proteins. (a) Expression of the target transcripts in relation to GAPDH measured for each cell line independently. (b) Expression of the target transcripts normalized to that of Jurkat cells. Data represent mean and S.E. of two independent experiments; statistical analysis was performed using two-way analysis of variances, and is shown only for gene expression above the threshold of ±twofold of Jurkat expression; *** = $p < 0.001$; n.d. = none determined, SKM = SK-MEL-28.

values were normalized to these of each respective untreated cells. Again, many significant changes were observed, but only those showing a ±twofold increase or decrease were labeled. In Jurkat cells, argon plasma treatment significantly increased thioredoxin (TXN) and HMOX1 expression and decreased TXNRD1 copy numbers [Fig. 3(a)]. For He/O_2, also

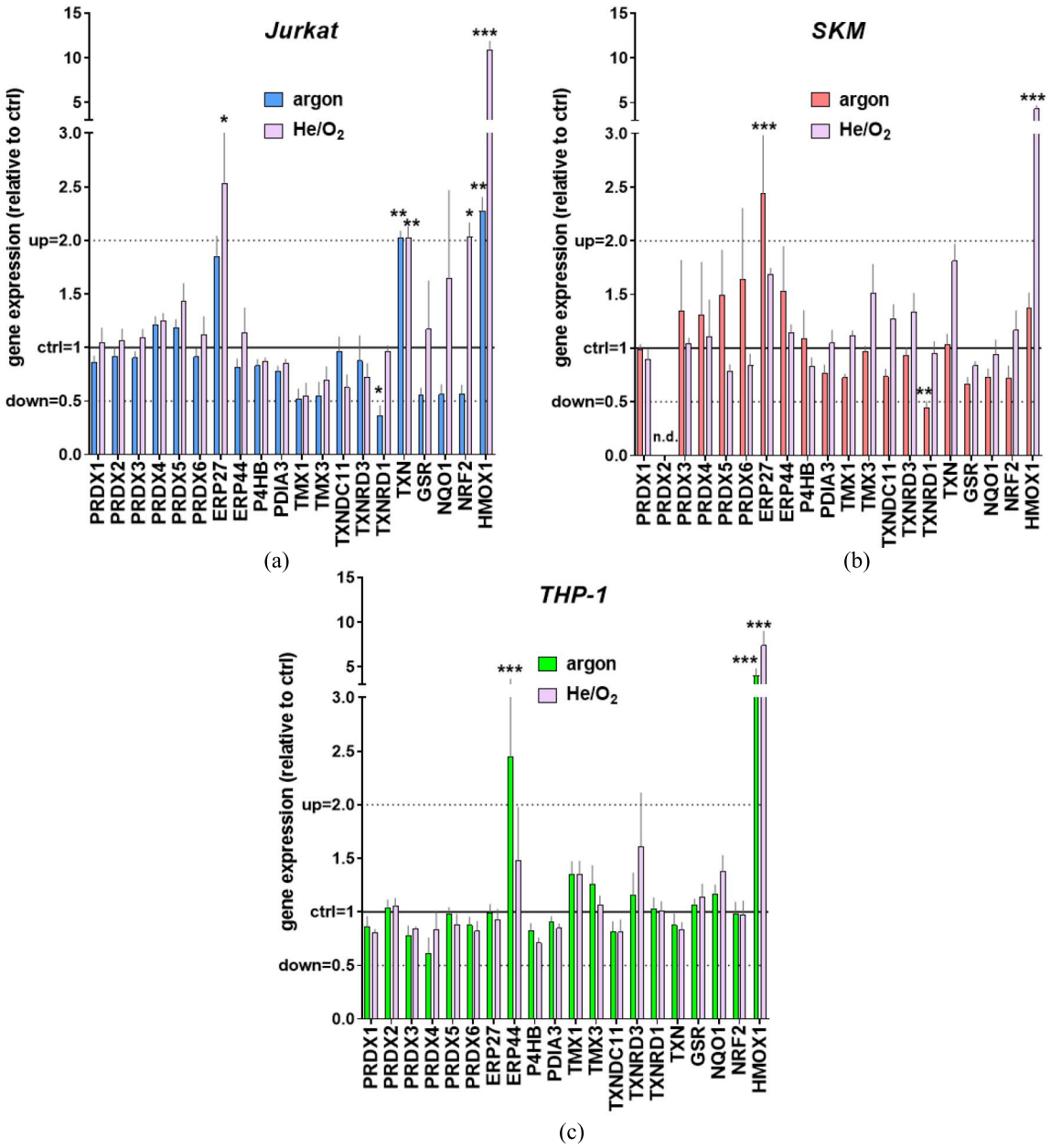

Fig. 3. Only HMOX1 was commonly regulated upon plasma treatment across the three different cell lines investigated. (a)–(c) Control-normalized gene expression of transcripts coding for 20 redox-related proteins in (a) Jurkat, (b) SKM, and (c) THP-1 cells at 4 h following treatment (30 s) with either argon or He/O_2 plasma. Data represent mean and S.E. of two independent experiments; statistical analysis was performed using two-way analysis of variances, and is shown only for gene expression above the threshold of ± twofold of expression in untreated (control) cells; * = $p < 0.05$, ** = $p < 0.01$, *** = $p < 0.001$; n.d. = none determined, ctrl = control.

endoplasmic reticulum protein 27 (ERP27) and nuclear factor erythroid 2-related factor 2 (NRF2) regulating the expression of antioxidant proteins such as HMOX1, were significantly upregulated. In SKM cells, argon plasma treatment significantly increased ERP27 and decreased TXNRD1 expression, while He/O_2 also increased the number of HMOX1 transcripts [Fig. 3(b)]. In THP-1 cells, argon treatment significantly upregulated ERP44 and HMOX1, with the latter also being observed with He/O_2 treatment [Fig. 3(c)]. These data provided evidence that several redox-regulated protein transcripts were part of the oxidative stress response evoked by plasma treatment. Of the 13 significant changes observed, five related to HMOX1. HMOX1 was the only gene showing a consistent increase in all three cell types and the two feed gas conditions investigated.

C. Knockdown of HO-1 and IL8 Augmented the Plasma-Mediated Cytotoxicity

The qPCR screen identified HMOX1 as a collective response element to plasma treatment. We next aimed at siRNA-mediated knockdown to understand its putative role in cytotoxic responses to plasma treatment. The protein of HMOX1, heme oxygenase 1 (HO-1) is co-expressed with

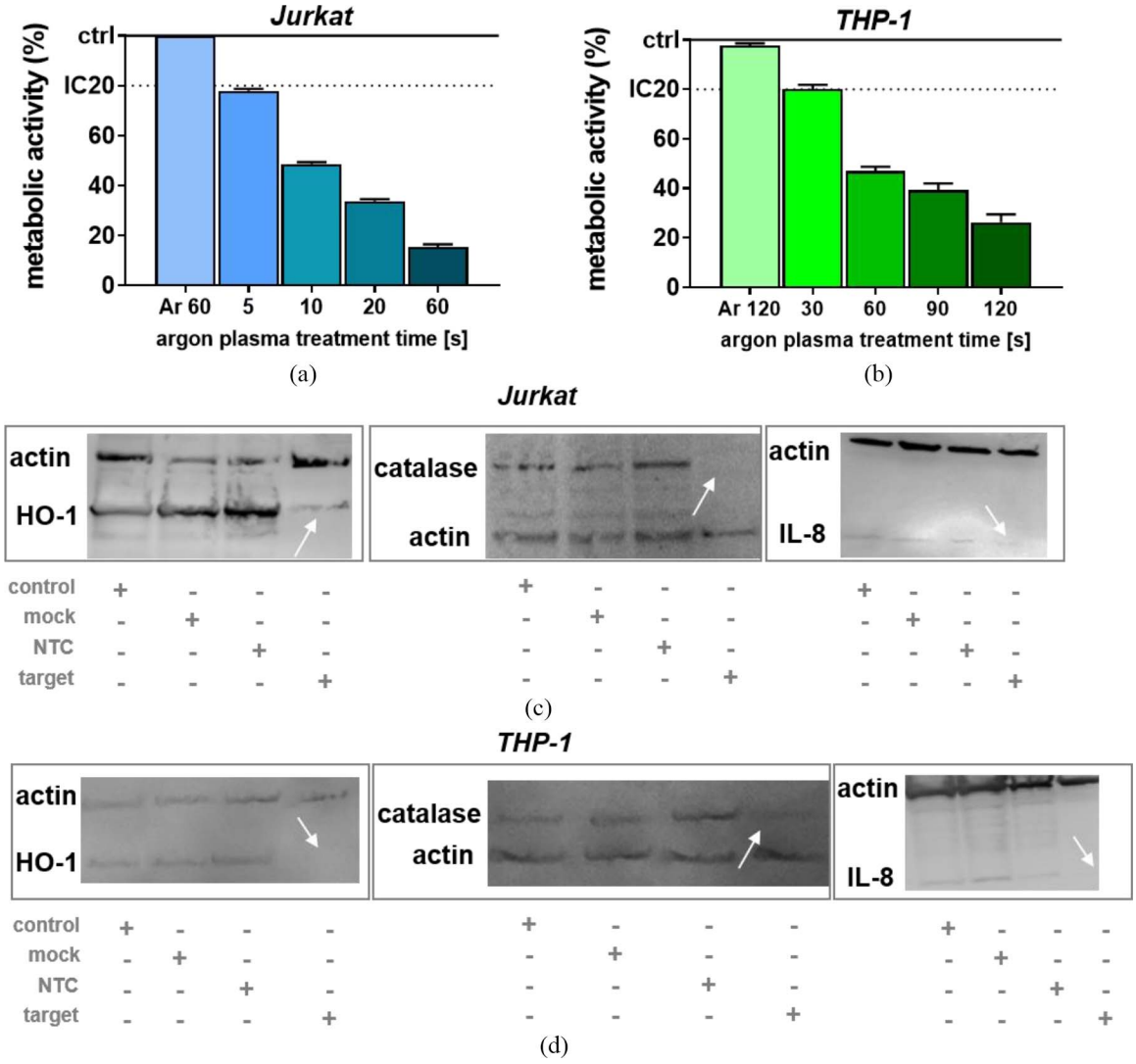

Fig. 4. Determination of IC20 treatment times and confirmation of target protein knockdown using siRNA. (a) Jurkat and (b) THP-1 cells were exposed to argon plasma treatment or argon gas control (Jurkat: 60 s; THP-1: 120 s), before assessing their metabolic activity and IC20 (Jurkat: 5 s; THP-1: 30 s) at 24 h. (c) and (d) Validation of protein knockdown via siRNA in Jurkat (c) and THP-1 (d) cells for the proteins HO-1, catalase, and IL8. Data represent mean and S.E. or are representative of two independent experiments. Mock = transfection without target siRNA, NTC = nontargeting control (luciferase), HO-1 = heme oxygenase 1 protein, IL8 = interleukin 8, Ar = argon gas only control. MW are 42 kDa (actin), 14 kDa (HO-1), 58 kDa (catalase), and 11 kDa (IL8).

catalase [56] and chemokine IL8 [57] whose expression was knocked down as well.

Catalase decomposes H_2O_2, an oxidant frequently observed as a long-lived product in plasma-treated liquids. IL8 appeared attractive because of its 40-fold higher expression in THP-1 cells as compared to Jurkat cells [58]. The SKM melanoma cells were omitted because we could not apply the same transfection protocol as used for Jurkat and THP-1 cells. Only argon plasma treatment was used to reduce the number of iterations. To allow for comparison of reduction rates in metabolic activity, the plasma treatment time decreasing the metabolic activity by 20% (IC20) was identified in Jurkat cells being 5 s [Fig. 4(a)] and THP-1 cells being 30 s [Fig. 4(b)]. Treatment with argon gas alone (plasma: off) showed no effect. The knockdown efficiency of the target proteins was confirmed 24 h after transfection in Jurkat [Fig. 4(c)] and THP-1 cells [Fig. 4(d)] via Western Blot.

Next, the effect of plasma treatment was identified 24 h after exposure. Several conditions were used, including untreated (not transfected, not plasma-treated), mock transfected (transfection, but without siRNA), NTC transfected (transfected with siRNA but targeting a nonexisting target in cells, the enzyme luciferase), and the target transfection with siRNA inhibiting either HMOX1, catalase (CAT), or IL8 (Fig. 5). The metabolic activity was normalized to that of untreated cells. Each of the procedures (the transfection, the insertion of siRNA, and the plasma treatment) has its individual degree of cytotoxic effect that cumulates when several of the procedures are combined, as shown for Jurkat cells [Fig. 5(a)]. To compare any additive or synergistic effect of the plasma treatment and the transfection with the target, the mean decrease in metabolic activity is given in yellow numbers. The sum of the single treatments (plasma, and transfection with target siRNA) is shown in parentheses (e.g., for HMOX1: plasma 17.6% plus

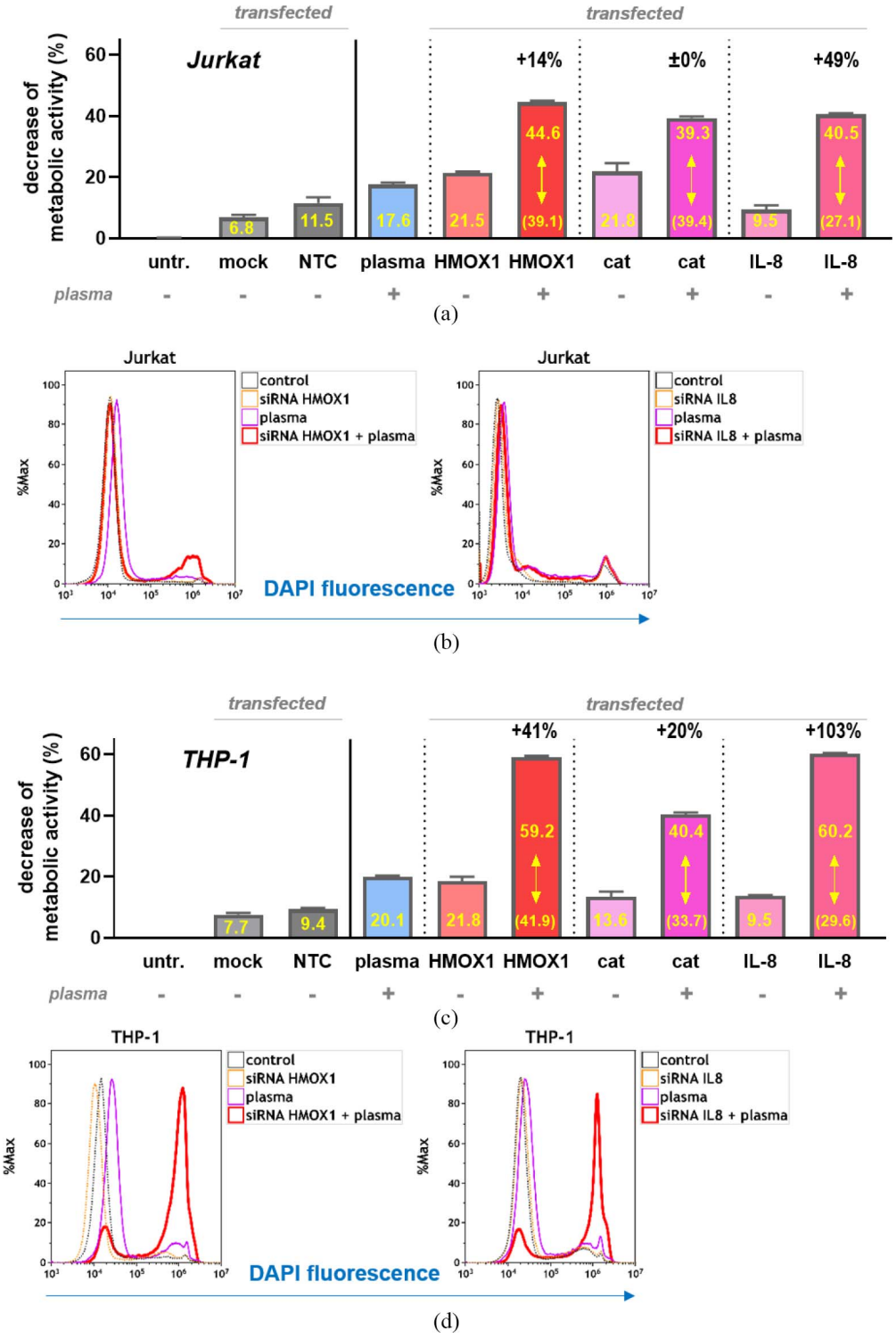

Fig. 5. Knockdown of HO-1 and IL8 exacerbated the cytotoxicity of plasma treatment in leukemia cells. (a) and (b) Decrease of metabolic activity normalized to untreated cells (a) and flow cytometry (b) of terminally dead ($DAPI^+$) at 24 h of Jurkat cells either left untreated (untr.) or transfected without (mock) and with a siRNA targeting a nonexpressed mRNA (nontargeting control, NTC = luciferase) or target (HMOX1, CAT, IL8) transcript with or without subsequent exposure to argon plasma. (c) and (d) metabolic activity (c) and flow cytometry (d) of terminally dead ($DAPI^+$) at 24 h of THP-1 cells either left untreated (untr.) or transfected without (mock) and with a siRNA targeting a nonexpressed mRNA (nontargeting control, NTC = luciferase) or target (HMOX1, CAT, IL8) transcript with or without subsequent exposure to argon plasma. Data represent mean and S.E. of four experiments with yellow numbers (a) and (c) indicating the mean of each bar, and the yellow numbers in parentheses indicating the sum of the reduction via plasma alone (blue graphs) and each of the targets without plasma treatment. The arrows point to the relevant comparisons. HO-1 = heme oxygenase 1 protein, IL8 = interleukin 8, and CAT = catalase.

HMOX1 without plasma 21.5% equals 39.1%), to allow comparison against the combination treatment (plasma and transfection with siRNA targeting HMOX1 being 44.6%). This way, we identified the knockdown of HMOX1 (to a minor extent) and IL8 (to a major extent) but not catalase to yield elevated toxicity in plasma-treated Jurkat cells. This was confirmed for

HMOX1 and IL8 by flow cytometry, assessing the distribution of DAPI as an indicator of terminally dead Jurkat cells [Fig. 5(b)]. In plasma-treated THP-1 cells, suppression of each of the targets led to a more pronounced synergistic decrease in metabolic activity, with HMOX1 knockdown doubling the cytotoxic plasma effect [Fig. 5(c)]. This was confirmed for HMOX1 and IL8 by flow cytometry, assessing the distribution of DAPI as an indicator of terminally dead THP-1 cells [Fig. 5(d)].

D. IL8 Receptor Blockage Augmented HO-1 and Partially IL8 Secretion as Well as Plasma-Induced Cytotoxicity in Leukemia Cells

Of the three targets investigated, knockdown of IL8 showed the most substantial effects in the two leukemia cell lines investigated. The chemokine CXCL8 (IL8) is usually released into the extracellular space where it can bind to its receptors, CD181 (CXCR1) and CD182 (CXCR2), on cells. Both receptors were highly expressed on both Jurkat and THP-1 cells [Fig. 6(a)]. As the knockdown of IL8 provided increased cytotoxicity with plasma treatment, we hypothesized IL8 to act as a pro-survival signal that might be correlated with increased IL8-receptor expression in response to plasma-induced oxidative stress. To our surprise, both CD181 and CD182 were significantly downregulated in the viable ($DAPI^-$) cell fraction 24 h after plasma treatment in both Jurkat [Fig. 6(b)] and THP-1 [Fig. 6(c)] cells. To vice versa test the effect of exogenous recombinant IL8 and IL8-receptor (CD181/CD181) blockage, Jurkat and THP-1 cells preincubated with IL8 or anti CD181/CD182 antibodies, exposed to plasma, incubated for 24 h, and analyzed for cell viability. Jurkat viability declined with antibody treatment to a greater extent compared to plasma exposure alone [Fig. 6(e)], while IL8 neither rescued nor elevated plasma-induced cell death [Fig. 6(f)]. Additive cytotoxicity of the antibody treatment was even more pronounced in THP-1 cells [Fig. 6(g)], while the addition of IL8 here also failed to change the amplitude of plasma-induced cytotoxicity [Fig. 6(h)]. The IL8-receptor blockage also induced a significantly increased IL8 release in THP-1 but not Jurkat cells, which was further elevated with plasma treatment [Fig. 6(i)]. For HO-1, a significant increase in its secretion levels was found with IL8 receptor blockage in both untreated Jurkat [Fig. 6(j)] and THP-1 cells [Fig. 6(k)]. Plasma treatment, however, did not elevate HO-1 secretion in either of the cell types, while the addition of IL8 decreased HO-1 release in Jurkat and increased HO-1 release in THP-1 cell, although to a minor extent.

IV. Discussion

In the present study, we aimed at identifying both the most cytotoxic plasma feed gas composition and the molecular basis of plasma-mediated cytotoxicity in a proof-of-concept study using two leukemia cell lines. Overall, Jurkat cells were more sensitive to plasma-induced cell death compared to THP-1 cells. Argon (but not He/O_2) plasma treatment showed the most substantial toxicity against Jurkat, whereas He/O_2 (but not argon) plasma treatment showed the strongest toxicity in THP-1 cells. Knockdown of the proteins HO-1 and IL8, as well as IL8-receptor blockage, augmented cytotoxic plasma effects in both cell lines, suggesting a positive feedback loop between ROS-induced HO-1 expression, IL8 release, and binding of IL8 to IL8 receptors providing pro-survival signaling.

IL8 is a chemokine alarming leukocytes to infiltrate inflamed tissues [59], [60]. It is produced by several types of cells, including immune cells [61], [62] and stromal cells [63], [64], and induces calcium signaling and leukocyte maturation [65], [66] as well as angiogenesis [67]. Oxidative stress, as induced by plasma-derived ROS, increases IL8 secretion in many cell types, including dendritic cells [68], endothelial cells [67], and monocytes [69]. With plasma treatment, we have recently shown an increase of IL8 mRNA and release in THP-1 monocytes [70], even up to four days after treatment [71]. Plasma treatment also increases IL8 production in human keratinocytes [72], [73]. As a mechanism, an intracellular loss of potassium with subsequent MAPK/ERK activation is discussed that governs the IL8 secretory response upon plasma treatment [74]. Increased IL8 release has also been observed in plasma-treated human neutrophils [75] and ovarian cancer cells [15]. While there is ample evidence supporting the oxidative stress-dependent IL8 release in human cells, studies describing its mechanism of making cells more resilient to ROS-induced cell death, as shown in our study, are scarce. Besides MAPK-regulation, IL8 promoter hyperacetylation is suggested as one mechanism of action in response to oxidative stress [76]. Another frequently mentioned link between oxidative stress and IL8 release is the protein heme oxygenase 1 (HO-1) that can be activated through the transcription factor nuclear factor erythroid 2–Nrf2, eventually facilitating potent antioxidative responses [77].

The suppression of HO-1 potentiated plasma-mediated cytotoxic effects in our study. Vice versa, HO-1 was shown to extensively promote resistance to oxidative stress and protection from ROS-induced damage [78], [79]. The primary role of HO-1 is to degrade heme, thereby generating iron, biliverdin, and carbon monoxide [80]. While the importance of HO-1 in antioxidant defense in health and disease in undisputed [77], it is clear that cell cultures do not contain significant amounts of heme as in blood, making the exact mechanism of protection *in vitro* to remain largely elusive as of now. The mRNA of HO-1, HMOX1, is found to be frequently upregulated in response to oxidative stress in general and plasma treatment specifically. Underlining the results of this study, we have recently identified HMOX1 to serve as a common response element to plasma-induced oxidative stress in eight human cancer cell lines [14]. We found the target not only to be increased in plasma-treated monocytes [70] and keratinocytes [81] but also in plasma-treated acute wounds in mice, showing a 200-fold increase as compared to untreated wounds [3]. These data warrant more research on HMOX1/HO-1 expression being clear indicators for signaling responses to plasma-derived ROS in plasma medicine.

Another presumably obvious target to investigate is catalase. The enzyme detoxifies H_2O_2 at compelling rate

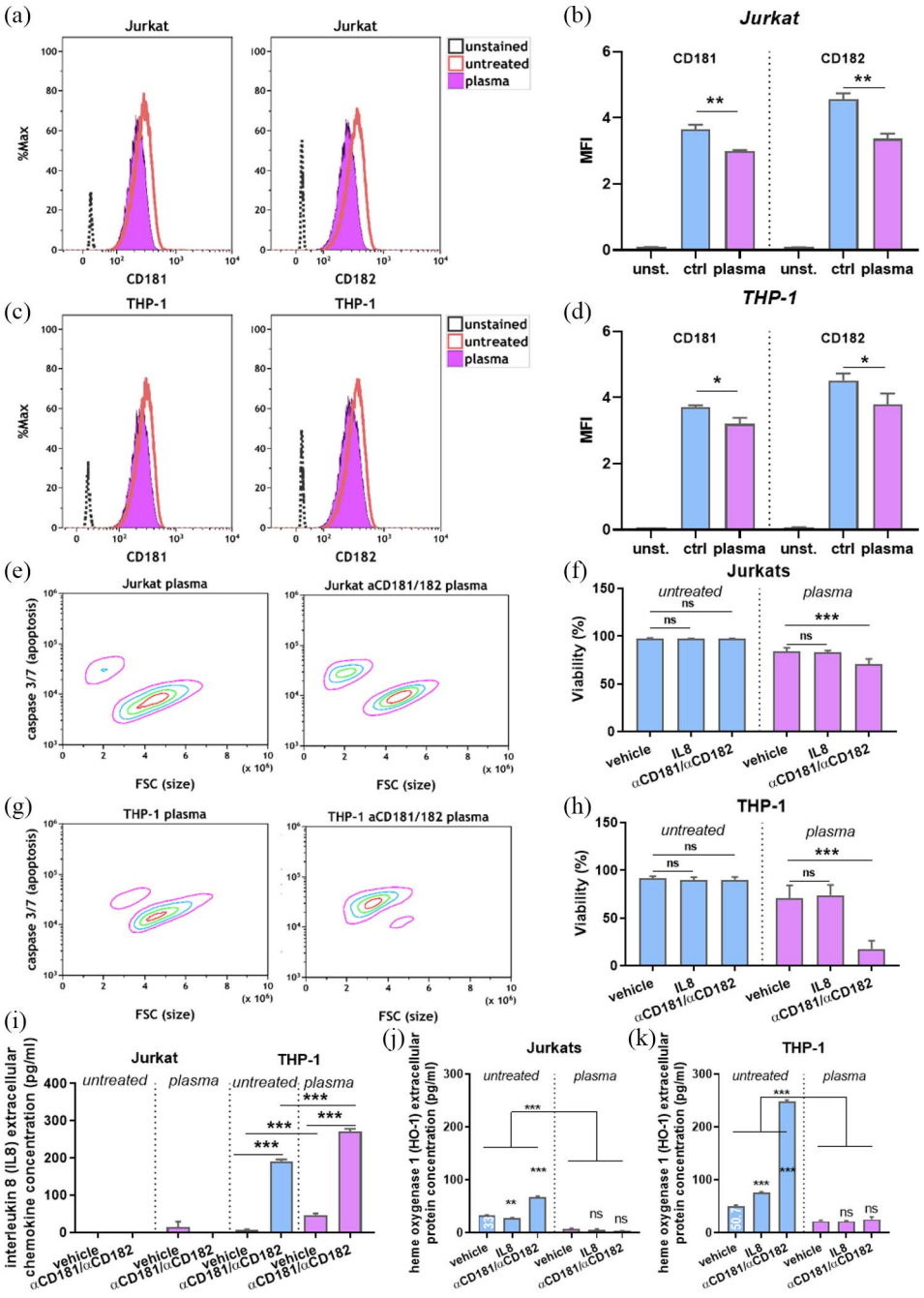

Fig. 6. IL8 receptor blockage augmented HO-1 and partially IL8 secretion as well as plasma-induced cytotoxicity in leukemia cells. (a)–(d) Representative overlay histograms of the fluorescence intensities of labeled CD181 and CD182 on viable (DAPI-) Jurkat cells (a) and quantification thereof (b), and DAPI- THP-1 cells (c) and quantification thereof (d) at 24 h following plasma treatment. (e) and (f) Representative dot-plot of the forward scatter (FSC, size) and the fluorescence intensity of caspase 3/7 activation in Jurkat cells indicative of apoptosis (e) and quantification of the percentage of viable cells in samples preincubated for 24 h with either vehicle, recombinant IL8 (100 ng/ml), or anti CD181/182 antibodies (f). (g) and (h) Representative dot-plot of the forward scatter (FSC, size) and the fluorescence intensity of caspase 3/7 activation in THP-1 cells indicative of apoptosis (g) and quantification of the percentage of viable cells in samples preincubated for 24 h with either vehicle, recombinant IL8 (100 ng/ml), or anti CD181/182 antibodies (h). (i) IL8, (j) HO-1, and (k) ELISA performed from the supernatants of the cells presented in (f) and (h). Data represent mean and S.E. of two to four independent experiments; statistical analysis was performed using t-test; * = $p < 0.05$, ** = $p < 0.01$; *** = $p < 0.001$; ctrl = control, unst. = unstained.

constants [82] but is restricted primarily to peroxisomes in cells. With plasma-derived ROS unlikely diffusing through several cell membranes and the cytosol without losing reactivity at the biomolecules present [33], the importance of this enzyme in plasma medicine is maybe overstated. It is also proposed that not the total levels of catalase but its location on the membrane might be decisive for antitumor plasma effects [83], [84]. Nevertheless, knockdown of catalase increased plasma-induced cytotoxicity in THP-1 cells to some extent in our study. One hypothesis might be that both HO-1 and catalase not only protect from plasma-derived ROS but also ROS being produced endogenously by the cells following plasma treatment. Several studies have mentioned endogenous ROS production in response to plasma exposure [85], [86].

At higher concentrations, ROS damage cells, leading to their demise. However, it is currently unclear whether the types or amounts of ROS or both govern their cytotoxic responses. For instance, different cell types may have different sensitivities to the ROS-induced cell death, independent of the type of ROS being used. We here provide evidence for the opposite case. The argon plasma regimen is rich in the generation of hydroxyl radicals [87], ultimately decomposing to H_2O_2. By contrast, the He/O_2 condition was proposed to be rich in atomic and singlet delta oxygen [88], [89], with the former facilitating the generation of hypochlorous acid [38], provided extensive disturbances do not lead to quenching via ambient-air derived oxygen to ozone [51]. Using a different plasma jet than the kINPen, we have previously established the high sensitivity of THP-1 cells to He/O_2 plasma [40]. For Jurkat T-lymphocytes, we expected a similar tendency. However, He/O_2 plasma was among the least cytotoxic condition in Jurkat cells, while argon plasma showed the highest efficacy. By contrast, all helium plasma conditions were more cytotoxic in THP-1 cells as compared to the argon plasma treatment. These results drastically change our view of ROS-induced cell death in plasma medicine and in redox biology. While several studies [90]–[92], including our own [6], [14], [23], [44], [93], have identified some cell lines to more susceptible to plasma treatment over others, using different plasma-derived ROS compositions might have yielded opposite effects, as suggested with our results observed here in Jurkat and THP-1 cells. The broader implications of these findings remain to be established but it can be hypothesized that tumors unresponsive to one type of plasma might become responsive when changing the ROS composition in the very same device. Hence, it can be claimed that identifying optimal ROS compositions for each of the targeted tumor entities is a challenge that only has started to be tackled in the field of plasma medicine.

Plasma treatment led to a significant decrease in the expression in the surface receptors CXCR1 (CD181) and CXCR2 (CD182) known to bind IL8 [94]. This might be due to the oxidation-induced change of epitopes, and subsequent differences in antibody binding. However, it is more likely that this downregulation is a consequence of a response to stimulus, as both CD181 and CD182 are rapidly internalized and recycled upon target binding to allow desensitization to IL8 for migrating along the chemokine gradient in tissues [95]. Our data are in line with this as plasma treatment induced a slight (Jurkat) and prominent (THP-1) induction of IL8 release, which in turn leads to internalization of the receptors. However, CD181/CD182 expression can also be modulated in response to infection [96]. CXCR2 is moreover upregulated in many types of cancers to sustain inflammation and promote growth through the binding of several CXCL-ligands [97]. CD181/CD182 blockage with antibodies significantly augmented the plasma-induced cell death in both leukemia lines tested. This validates the importance of the CXCL8-axis in the survival of these cells in response to plasma-induced oxidative stress, a conclusion also drawn in previous studies on chemoresistance using human prostate cancer cells [98], [99]. Interestingly, both untreated and plasma-treated THP-1 cells attempted to counteract on the lack of autocrine IL8 stimulation due to the IL8R-blockage by increasing the production of IL8 more than 20-fold. In the combination with the massively elevated cell death observed with anti-CD181/CD182 treatment and siRNA-mediated IL8 knockdown, our functional data suggest the autocrine IL8 stimulation to be of so far unreported relevance in the coping of plasma-induced oxidative stress *in vitro*.

Heme oxygenase 1 (HO-1) undoubtedly is relevant in health in disease [100], [101]. The consequences of its regulation, however, are not linear, since modest upregulation is associated with antioxidative activity and cytoprotection while higher levels even promote ROS production [102], [103]. In human monocytes, HO-1 upregulation results in decrease TNFα and ROS levels, and increased SOD expression [104]. In oncology, it is known that HO-1 expression increases angiogenesis, chemoresistance, and protects from apoptosis [105]. Hence, the substantial increase in cell death observed in HO-1 knockdown experiments was not surprising, while the role of IL8 in such setting is less clear. This is further complicated as IL8 release depends on other factors, such as HIF-1α attenuating Nrf2-dependent IL8 production. Nevertheless, expression of IL8 is independent on that of HO-1 [57]. Our data hence suggest that co-suppression of both HO-1 and IL-8 might further amplify plasma-induced toxicity. The therapeutic relevance of this, however, remains to be established.

V. Conclusion

In our proof-of-concept study using two leukemia cell lines, the plasma-induced cytotoxicity depended on both the cell type investigated and the ROS-mixtures generated. While the exact mechanisms of cells succumbing to plasma-induced cell death remain elusive, we provide evidence that both heme oxygenase 1 and interleukin 8, as well as autocrine stimulation via the two IL8-receptors, promote the survival of plasma-treated cells. Further research is warranted to understand the broader implications of these findings in the fields of plasma medicine and plasma onco-therapy.

Acknowledgment

The authors would like to thank Maxi Lippert, Melissa Mühl, and Kan-Kau Chow, who provided technical support with the metabolic activity assays, and the gene expression and transfection experiments.

References

[1] S. Bekeschus, A. Schmidt, K.-D. Weltmann, and T. von Woedtke, "The plasma jet kINPen—A powerful tool for wound healing," *Clin. Plasma Med.*, vol. 4, no. 1, pp. 19–28, 2016.

[2] G. Isbary *et al.*, "Successful and safe use of 2 min cold atmospheric argon plasma in chronic wounds: Results of a randomized controlled trial," *Brit. J. Dermatol.*, vol. 167, no. 2, pp. 404–410, Aug. 2012.

[3] A. Schmidt, T. von Woedtke, B. Vollmar, S. Hasse, and S. Bekeschus, "NRF2 signaling and inflammation are key events in physical plasma-spurred wound healing," *Theranostics*, vol. 9, no. 4, pp. 1066–1084, 2019.

[4] J. Schlegel, J. Köritzer, and V. Boxhammer, "Plasma in cancer treatment," *Clin. Plasma Med.*, vol. 1, no. 2, pp. 2–7, 2013.

[5] S. Bekeschus *et al.*, "*Ex vivo* exposure of human melanoma tissue to cold physical plasma elicits apoptosis and modulates inflammation," *Appl. Sci.*, vol. 10, no. 6, p. 1971, 2020.

[6] S. Bekeschus *et al.*, "Risk assessment of kINPen plasma treatment of four human pancreatic cancer cell lines with respect to metastasis," *Cancers*, vol. 11, no. 9, p. 1237, Aug. 2019.

[7] L. Brulle *et al.*, "Effects of a non thermal plasma treatment alone or in combination with gemcitabine in a MIA $PaCa_2$-luc orthotopic pancreatic carcinoma model," *PLoS ONE*, vol. 7, no. 12, Dec. 2012, Art. no. e52653.

[8] K. R. Liedtke *et al.*, "Cold physical plasma selectively elicits apoptosis in murine pancreatic cancer cells *in vitro* and *in ovo*," *Anticancer Res.*, vol. 38, no. 10, pp. 5655–5663, Oct. 2018.

[9] S. Bekeschus *et al.*, "Environmental control of an argon plasma effluent and its role in THP-1 monocyte function," *IEEE Trans. Plasma Sci.*, vol. 45, no. 12, pp. 3336–3341, Dec. 2017.

[10] C. Wang *et al.*, "The relation between doses or post-plasma time points and apoptosis of leukemia cells induced by dielectric barrier discharge plasma," *AIP Adv.*, vol. 5, no. 12, Dec. 2015, Art. no. 127220.

[11] S. Bekeschus *et al.*, "Elevated H2AX phosphorylation observed with kINPen plasma treatment is not caused by ROS-mediated DNA damage but is the consequence of apoptosis," *Oxidative Med. Cellular Longevity*, vol. 2019, Jun. 2019, Art. no. 8535163.

[12] S. Bekeschus, M. Lippert, K. Diepold, G. Chiosis, T. Seufferlein, and N. Azoitei, "Physical plasma-triggered ROS induces tumor cell death upon cleavage of HSP90 chaperone," *Sci. Rep.*, vol. 9, no. 1, p. 4112, Mar. 2019.

[13] J. Lafontaine, J. S. Boisvert, A. Glory, S. Coulombe, and P. Wong, "Synergy between non-thermal plasma with radiation therapy and olaparib in a panel of breast cancer cell lines," *Cancers*, vol. 12, no. 2, p. 348, Feb. 2020.

[14] S. Bekeschus, E. Freund, K. Wende, R. K. Gandhirajan, and A. Schmidt, "$HMOX_1$ upregulation is a mutual marker in human tumor cells exposed to physical plasma-derived oxidants," *Antioxidants*, vol. 7, no. 11, p. 151, Oct. 2018.

[15] S. Bekeschus *et al.*, "Plasma treatment of ovarian cancer cells mitigates their immuno-modulatory products active on THP-1 monocytes," *Plasma*, vol. 1, no. 1, pp. 201–217, 2018.

[16] A. Bisag *et al.*, "Plasma-activated ringer's lactate solution displays a selective cytotoxic effect on ovarian cancer cells," *Cancers*, vol. 12, no. 2, p. 476, 2020.

[17] D. Koensgen *et al.*, "Cold atmospheric plasma (CAP) and CAP-stimulated cell culture media suppress ovarian cancer cell growth—A putative treatment option in ovarian cancer therapy," *Anticancer Res.*, vol. 37, no. 12, pp. 6739–6744, Dec. 2017.

[18] J. Moritz, H.-R. Metelmann, and S. Bekeschus, "Physical plasma treatment of eight human cancer cell lines demarcates upregulation of CD112 as a common immunomodulatory response element," *IEEE Trans. Radiat. Plasma Med. Sci.*, vol. 4, no. 3, pp. 343–349, Mar. 2020.

[19] D. Han *et al.*, "Antitumorigenic effect of atmospheric-pressure dielectric barrier discharge on human colorectal cancer cells via regulation of Sp1 transcription factor," *Sci. Rep.*, vol. 7, Feb. 2017, Art. no. 43081.

[20] E. Freund *et al.*, "Physical plasma-treated saline promotes an immunogenic phenotype in CT26 colon cancer cells *in vitro* and *in vivo*," *Sci. Rep.*, vol. 9, no. 1, p. 634, Jan. 2019.

[21] G. Pasqual-Melo *et al.*, "Combination of gas plasma and radiotherapy has immunostimulatory potential and additive toxicity in murine melanoma cells *in vitro*," *Int. J. Mol. Sci.*, vol. 21, no. 4, p. 1379, 2020.

[22] B. B. Choi, M. S. Kim, U. K. Kim, J. W. Hong, H. J. Lee, and G. C. Kim, "Targeting NEU protein in melanoma cells with non-thermal atmospheric pressure plasma and gold nanoparticles," *J. Biomed. Nanotechnol.*, vol. 11, no. 5, pp. 900–905, May 2015.

[23] S. Bekeschus *et al.*, "xCT (SLC7A11) expression confers intrinsic resistance to physical plasma treatment in tumor cells," *Redox Biol.*, vol. 30, Feb. 2020, Art. no. 101423.

[24] S. Hasse *et al.*, "Cold argon plasma as adjuvant tumour therapy on progressive head and neck cancer: A preclinical study," *Appl. Sci.*, vol. 9, no. 10, p. 2061, May 2019.

[25] S. U. Kang *et al.*, "Nonthermal plasma induces head and neck cancer cell death: the potential involvement of mitogen-activated protein kinase-dependent mitochondrial reactive oxygen species," *Cell Death Disc.*, vol. 5, no. 2, Feb. 2014, Art. no. e1056.

[26] J. Berner *et al.*, "Medical gas plasma treatment in head and neck cancer—Challenges and opportunities," *Appl. Sci.*, vol. 10, no. 6, p. 1944, 2020.

[27] M. Akter, A. Jangra, S. A. Choi, E. H. Choi, and I. Han, "Non-thermal atmospheric pressure bio-compatible plasma stimulates apoptosis via p38/MAPK mechanism in U87 malignant glioblastoma," *Cancers*, vol. 12, no. 1, p. 245, Jan. 2020.

[28] Z. Chen *et al.*, "A novel micro cold atmospheric plasma device for glioblastoma both *in vitro* and *in vivo*," *Cancers*, vol. 9, no. 6, p. 61, May 2017.

[29] G. Daeschlein *et al.*, "Enhanced anticancer efficacy by drug chemotherapy and cold atmospheric plasma against melanoma and glioblastoma cell lines *In Vitro*," *IEEE Trans. Radiat. Plasma Med. Sci.*, vol. 2, no. 2, pp. 153–159, Jan. 2018.

[30] H.-R. Metelmann *et al.*, "Clinical experience with cold plasma in the treatment of locally advanced head and neck cancer," *Clin. Plasma Med.*, vol. 9, pp. 6–13, Mar. 2018.

[31] H. R. Metelmann, C. Seebauer, R. Rutkowski, M. Schuster, S. Bekeschus, and P. Metelmann, "Treating cancer with cold physical plasma: On the way to evidence-based medicine," *Contrib. Plasma Phys.*, vol. 58, no. 5, pp. 415–419, Jun. 2018.

[32] K. Witzke *et al.*, "Plasma medical oncology: Immunological interpretation of head and neck squamous cell carcinoma," *Plasma Process. Polym.*, Mar. 2020, Art. no. e1900258.

[33] A. Privat-Maldonado *et al.*, "ROS from physical plasmas: Redox chemistry for biomedical therapy," *Oxidative Med. Cellular Longevity*, vol. 2019, Oct. 2019, Art no. 9062098.

[34] J. Winter, R. Brandenburg, and K. D. Weltmann, "Atmospheric pressure plasma jets: An overview of devices and new directions," *Plasma Sources Sci. Technol.*, vol. 24, no. 6, Dec. 2015, Art. no. 064001.

[35] A. Schmidt-Bleker, J. Winter, A. Bosel, S. Reuter, and K. D. Weltmann, "On the plasma chemistry of a cold atmospheric argon plasma jet with shielding gas device," *Plasma Sources Sci. Technol.*, vol. 25, no. 1, Feb. 2016, Art. no. 015005.

[36] J. Benedikt *et al.*, "Absolute OH and O radical densities in effluent of a He/H_2O micro-scaled atmospheric pressure plasma jet," *Plasma Sources Sci. Technol.*, vol. 25, no. 4, Aug. 2016, Art. no. 045013.

[37] S. Bekeschus, A. Schmidt, F. Niessner, T. Gerling, K. D. Weltmann, and K. Wende, "Basic research in plasma medicine—A throughput approach from liquids to cells," *J. Visual. Exp.*, vol. 129, Nov. 2017, Art. no. e56331.

[38] K. Wende *et al.*, "Identification of the biologically active liquid chemistry induced by a nonthermal atmospheric pressure plasma jet," *Biointerphases*, vol. 10, no. 2, Jun. 2015, Art. no. 029518.

[39] H. Jablonowski *et al.*, "Plasma jet's shielding gas impact on bacterial inactivation," *Biointerphases*, vol. 10, no. 2, Jun. 2015, Art. no. 029506.

[40] S. Bekeschus *et al.*, "Oxygen atoms are critical in rendering THP-1 leukaemia cells susceptible to cold physical plasma-induced apoptosis," *Sci. Rep.*, vol. 7, no. 1, p. 2791, Jun. 2017.

[41] J. Winter *et al.*, "Tracking plasma generated H_2O_2 from gas into liquid phase and revealing its dominant impact on human skin cells," *J. Phys. D Appl. Phys.*, vol. 47, no. 28, Jul. 2014, Art. no. 285401.

[42] S. Bekeschus, C. Seebauer, K. Wende, and A. Schmidt, "Physical plasma and leukocytes—Immune or reactive?," *Biol. Chem.*, vol. 400, no. 1, pp. 63–75, Dec. 2018.

[43] L. Bundscherer *et al.*, "Viability of human blood leukocytes compared with their respective cell lines after plasma treatment," *Plasma Med.*, vol. 3, nos. 1–2, pp. 71–80, 2013.

[44] K. Wende, S. Reuter, T. von Woedtke, K. D. Weltmann, and K. Masur, "Redox-based assay for assessment of biological impact of plasma treatment," *Plasma Process. Polym.*, vol. 11, no. 7, pp. 655–663, Jul. 2014.

[45] S. Reuter, T. von Woedtke, and K. D. Weltmann, "The kINPen—A review on physics and chemistry of the atmospheric pressure plasma jet and its applications," *J. Phys. D Appl. Phys.*, vol. 51, no. 23, Jun. 2018, Art. no. 233001.

[46] M. Dunnbier *et al.*, "Ambient air particle transport into the effluent of a cold atmospheric-pressure argon plasma jet investigated by molecular beam mass spectrometry," *J. Phys. D Appl. Phys.*, vol. 46, no. 43, Oct. 2013, Art. no. 435203.

[47] H. Jablonowski, A. Schmidt-Bleker, K. D. Weltmann, T. von Woedtke, and K. Wende, "Non-touching plasma-liquid interaction—Where is aqueous nitric oxide generated?" *Phys. Chem. Chem. Phys.*, vol. 20, no. 39, pp. 25387–25398, Oct. 2018.

[48] S. Reuter *et al.*, "From RONS to ROS: Tailoring plasma jet treatment of skin cells," *IEEE Trans. Plasma Sci.*, vol. 40, no. 11, pp. 2986–2993, Nov. 2012.

[49] A. Schmidt-Bleker, R. Bansemer, S. Reuter, and K.-D. Weltmann, "How to produce an NOx- instead of Ox-based chemistry with a cold atmospheric plasma jet," *Plasma Process. Polym.*, vol. 13, no. 11, pp. 1120–1127, 2016.

[50] A. Schmidt-Bleker *et al.*, "Propagation mechanisms of guided streamers in plasma jets: The influence of electronegativity of the surrounding gas," *Plasma Sources Sci. Technol.*, vol. 24, no. 3, May 2015, Art. no. 035022.

[51] A. Schmidt-Bleker, J. Winter, S. Iseni, M. Dunnbier, K. D. Weltmann, and S. Reuter, "Reactive species output of a plasma jet with a shielding gas device-combination of FTIR absorption spectroscopy and gas phase modelling," *J. Phys. D Appl. Phys.*, vol. 47, no. 14, Apr. 2014, Art. no. 145201.

[52] J. Winter, J. S. Sousa, N. Sadeghi, A. Schmidt-Bleker, S. Reuter, and V. Puech, "The spatio-temporal distribution of He (23S1) metastable atoms in a MHz-driven helium plasma jet is influenced by the oxygen/nitrogen ratio of the surrounding atmosphere," *Plasma Sources. Sci. Technol.*, vol. 24, no. 2, pp. 25015–25025, 2015.

[53] S. Bekeschus, R. Clemen, F. Niessner, S. K. Sagwal, E. Freund, and A. Schmidt, "Medical gas plasma jet technology targets murine melanoma in an immunogenic fashion," *Adv. Sci.*, vol. 7, no. 10, May 2020, Art. no. 1903438.

[54] S. Bekeschus *et al.*, "High throughput image cytometry micronucleus assay to investigate the presence or absence of mutagenic effects of cold physical plasma," *Environ. Mol. Mutagenesis*, vol. 59, no. 4, pp. 268–277, May 2018.

[55] E. M. Hanschmann, J. R. Godoy, C. Berndt, C. Hudemann, and C. H. Lillig, "Thioredoxins, glutaredoxins, and peroxiredoxins—Molecular mechanisms and health significance: From cofactors to antioxidants to redox signaling," *Antioxid. Redox Signal.*, vol. 19, no. 13, pp. 1539–1605, Nov. 2013.

[56] S. Turkseven *et al.*, "Antioxidant mechanism of heme oxygenase-1 involves an increase in superoxide dismutase and catalase in experimental diabetes," *Amer. J. Physiol. Heart Circuit Physiol.*, vol. 289, no. 2, pp. 701–707, Aug. 2005.

[57] A. Loboda *et al.*, "HIF-1 induction attenuates Nrf_2-dependent IL-8 expression in human endothelial cells," *Antioxid. Redox Signal.*, vol. 11, no. 7, pp. 1501–1517, Jul. 2009.

[58] A. Schmidt *et al.*, "Redox-regulation of activator protein 1 family members in blood cancer cell lines exposed to cold physical plasma-treated medium," *Plasma Process. Polym.*, vol. 13, no. 12, pp. 1179–1188, Dec. 2016.

[59] A. Harada, N. Sekido, T. Akahoshi, T. Wada, N. Mukaida, and K. Matsushima, "Essential involvement of interleukin-8 (IL-8) in acute inflammation," *J. Leukocyte Biol.*, vol. 56, no. 5, pp. 559–564, 1994.

[60] E. Engelhardt, A. Toksoy, M. Goebeler, S. Debus, E.-B. Bröcker, and R. Gillitzer, "Chemokines IL-8, GROα, MCP-1, IP-10, and Mig are sequentially and differentially expressed during phase-specific infiltration of leukocyte subsets in human wound healing," *Amer. J. Pathol.*, vol. 153, no. 6, pp. 1849–1860, 1998.

[61] A. E. Koch *et al.*, "Synovial tissue macrophage as a source of the chemotactic cytokine Il-8," *J. Immunol.*, vol. 147, no. 7, pp. 2187–2195, Oct. 1991.

[62] P. Scapini, J. A. Lapinet-Vera, S. Gasperini, F. Calzetti, F. Bazzoni, and M. A. Cassatella, "The neutrophil as a cellular source of chemokines," *Immunol. Rev.*, vol. 177, no. 1, pp. 195–203, Oct. 2000.

[63] R. E. Gerszten *et al.*, "MCP-1 and IL-8 trigger firm adhesion of monocytes to vascular endothelium under flow conditions," *Nature*, vol. 398, no. 6729, pp. 718–723, Apr. 1999.

[64] S. Tukaj, D. Gruner, D. Zillikens, and M. Kasperkiewicz, "Hsp90 blockade modulates bullous pemphigoid IgG-induced IL-8 production by keratinocytes," *Cell Stress Chaperones*, vol. 19, no. 6, pp. 887–894, Nov. 2014.

[65] W. Schorr, D. Swandulla, and H. U. Zeilhofer, "Mechanisms of IL-8-induced Ca2+ signaling in human neutrophil granulocytes," *Eur. J. Immunol.*, vol. 29, no. 3, pp. 897–904, Mar. 1999.

[66] N. Mukaida, A. Harada, and K. Matsushima, "Interleukin-8 (IL-8) and monocyte chemotactic and activating factor (MCAF/MCP-1), chemokines essentially involved in inflammatory and immune reactions," *Cytokine Growth Factor Rev.*, vol. 9, no. 1, pp. 9–23, Mar. 1998.

[67] A. Loboda, A. Jazwa, B. Wegiel, A. Jozkowicz, and J. Dulak, "Heme oxygenase-1-dependent and -independent regulation of angiogenic genes expression: Effect of cobalt protoporphyrin and cobalt chloride on VEGF and IL-8 synthesis in human microvascular endothelial cells," *Cell. Mol. Biol.*, vol. 51, no. 4, pp. 347–355, Sep. 2005.

[68] V. Verhasselt, M. Goldman, and F. Willems, "Oxidative stress up-regulates IL-8 and TNF-alpha synthesis by human dendritic cells," *Eur. J. Immunol.*, vol. 28, no. 11, pp. 3886–3890, Nov. 1998.

[69] C. P. Wong, E. J. Dashner-Titus, S. C. Alvarez, T. T. Chase, L. G. Hudson, and E. Ho, "Zinc deficiency and arsenic exposure can act both independently or cooperatively to affect zinc status, oxidative stress, and inflammatory response," *Biol. Trace Element Res.*, vol. 191, no. 2, pp. 370–381, Oct. 2019.

[70] S. Bekeschus *et al.*, "Redox stimulation of human THP-1 monocytes in response to cold physical plasma," *Oxidative Med. Cellular Longevity*, vol. 2016, Nov. 2016, Art. no. 5910695.

[71] E. Freund, J. Moritz, M. Stope, C. Seebauer, A. Schmidt, and S. Bekeschus, "Plasma-derived reactive species shape a differentiation profile in human monocytes," *Appl. Sci.*, vol. 9, no. 12, p. 2530, Jun. 2019.

[72] A. Schmidt *et al.*, "Non-thermal plasma treatment is associated with changes in transcriptome of human epithelial skin cells," *Free Radical Res.*, vol. 47, no. 8, pp. 577–592, Aug. 2013.

[73] A. Schmidt, S. Bekeschus, K. Jarick, S. Hasse, T. von Woedtke, and K. Wende, "Cold physical plasma modulates p53 and mitogen-activated protein kinase signaling in keratinocytes," *Oxidative Med. Cellular Longevity*, vol. 2019, pp. 1–16, Jan. 2019.

[74] E. Hotta, H. Hara, T. Kamiya, and T. Adachi, "Non-thermal atmospheric pressure plasma-induced IL-8 expression is regulated via intracellular K(+) loss and subsequent ERK activation in human keratinocyte HaCaT cells," *Archives Biochem. Biophys.*, vol. 644, pp. 64–71, Apr. 2018.

[75] S. Bekeschus *et al.*, "Neutrophil extracellular trap formation is elicited in response to cold physical plasma," *J. Leukocyte Biol.*, vol. 100, no. 4, pp. 791–799, Oct. 2016.

[76] T. R. Bartling and M. L. Drumm, "Oxidative stress causes IL8 promoter hyperacetylation in cystic fibrosis airway cell models," *Amer. J. Respiratory Cell Mol. Biol.*, vol. 40, no. 1, pp. 58–65, Jan. 2009.

[77] A. Loboda, M. Damulewicz, E. Pyza, A. Jozkowicz, and J. Dulak, "Role of Nrf_2/HO-1 system in development, oxidative stress response and diseases: An evolutionarily conserved mechanism," *Cellular Mol. Life Sci.*, vol. 73, no. 17, pp. 3221–3247, Sep. 2016.

[78] Y. C. Chen, J. M. Chow, C. W. Lin, C. Y. Wu, and S. C. Shen, "Baicalein inhibition of oxidative-stress-induced apoptosis via modulation of ERKs activation and induction of HO-1 gene expression in rat glioma cells C6," *Toxicol. Appl. Pharmacol.*, vol. 216, no. 2, pp. 263–273, Oct. 2006.

[79] H. Y. Lin, S. C. Shen, and Y. C. Chen, "Anti-inflammatory effect of heme oxygenase 1: Glycosylation and nitric oxide inhibition in macrophages," *J. Cell. Physiol.*, vol. 202, no. 2, pp. 579–590, Feb. 2005.

[80] G. Balla *et al.*, "Ferritin: A cytoprotective antioxidant strategem of endothelium," *J. Biol. Chem.*, vol. 267, no. 25, pp. 18148–18153, Sep. 1992.

[81] A. Schmidt, S. Bekeschus, H. Jablonowski, A. Barton, K. D. Weltmann, and K. Wende, "Role of ambient gas composition on cold physical plasma-elicited cell signaling in keratinocytes," *Biophys. J.*, vol. 112, no. 11, pp. 2397–2407, Jun. 2017.

[82] H. S. Marinho, L. Cyrne, E. Cadenas, and F. Antunes, "H_2O_2 delivery to cells: Steady-state versus bolus addition," *Methods Enzymol.*, vol. 526, pp. 159–173, Jun. 2013.

[83] G. Bauer, "Tumor cell-protective catalase as a novel target for rational therapeutic approaches based on specific intercellular ROS signaling," *Anticancer Res.*, vol. 32, no. 7, pp. 2599–2624, Jul. 2012.

[84] G. Bauer, "Increasing the endogenous NO level causes catalase inactivation and reactivation of intercellular apoptosis signaling specifically in tumor cells," *Redox Biol.*, vol. 6, pp. 353–371, Dec. 2015.

[85] K. Panngom, K. Y. Baik, M. K. Nam, J. H. Han, H. Rhim, and E. H. Choi, "Preferential killing of human lung cancer cell lines with mitochondrial dysfunction by nonthermal dielectric barrier discharge plasma," *Cell Death Disc.*, vol. 4, no. 5, p. e642, May 2013.

[86] X. Cheng, J. Sherman, W. Murphy, E. Ratovitski, J. Canady, and M. Keidar, "The effect of tuning cold plasma composition on glioblastoma cell viability," *PLoS ONE*, vol. 9, no. 5, 2014, Art. no. e98652.

[87] H. Jablonowski, R. Bussiahn, M. U. Hammer, K. D. Weltmann, T. von Woedtke, and S. Reuter, "Impact of plasma jet vacuum ultraviolet radiation on reactive oxygen species generation in bio-relevant liquids," *Phys. Plasmas*, vol. 22, no. 12, Dec. 2015, Art. no. 122008.

[88] D. Ellerweg, J. Benedikt, A. von Keudell, N. Knake, and V. Schulz-von der Gathen, "Characterization of the effluent of a He/O_2 microscale atmospheric pressure plasma jet by quantitative molecular beam mass spectrometry," *New J. Phys.*, vol. 12, no. 1, 2010, Art. no. 013021.

[89] S. Reuter, K. Niemi, V. Schulz-von der Gathen, and H. F. Dobele, "Generation of atomic oxygen in the effluent of an atmospheric pressure plasma jet," *Plasma Sources Sci. Technol.*, vol. 18, no. 1, Feb. 2009, Art. no. 015006.

[90] N. Kaushik *et al.*, "Non-thermal plasma with 2-deoxy-D-glucose synergistically induces cell death by targeting glycolysis in blood cancer cells," *Sci. Rep.*, vol. 5, p. 8726, Mar. 2015.

[91] R. Guerrero-Preston *et al.*, "Cold atmospheric plasma treatment selectively targets head and neck squamous cell carcinoma cells," *Int. J. Mol. Med.*, vol. 34, no. 4, pp. 941–946, Oct. 2014.

[92] E. Biscop *et al.*, "Influence of cell type and culture medium on determining cancer selectivity of cold atmospheric plasma treatment," *Cancers*, vol. 11, no. 9, p. 1287, Sep. 2019.

[93] D. Gumbel *et al.*, "Peroxiredoxin expression of human osteosarcoma cells is influenced by cold atmospheric plasma treatment," *Anticancer Res.*, vol. 37, no. 3, pp. 1031–1038, Mar. 2017.

[94] G. H. Fan, L. A. Lapierre, J. R. Goldenring, and A. Richmond, "Differential regulation of $CXCR_2$ trafficking by Rab GTPases," *Blood*, vol. 101, no. 6, pp. 2115–2124, Mar. 2003.

[95] R. Stillie, S. M. Farooq, J. R. Gordon, and A. W. Stadnyk, "The functional significance behind expressing two IL-8 receptor types on PMN," *J. Leukocyte Biol.*, vol. 86, no. 3, pp. 529–543, Sep. 2009.

[96] B. Schmausser *et al.*, "Downregulation of CXCR1 and CXCR2 expression on human neutrophils by Helicobacter pylori: A new pathomechanism in H. pylori infection?" *Infection Immunity*, vol. 72, no. 12, pp. 6773–6779, Dec. 2004.

[97] Y. Cheng, X. L. Ma, Y. Q. Wei, and X. W. Wei, "Potential roles and targeted therapy of the CXCLs/CXCR2 axis in cancer and inflammatory diseases," *Biochim Biophys Acta Rev Cancer*, vol. 1871, no. 2, pp. 289–312, Apr. 2019.

[98] C. Wilson *et al.*, "Chemotherapy-induced CXC-chemokine/CXC-chemokine receptor signaling in metastatic prostate cancer cells confers resistance to oxaliplatin through potentiation of nuclear factor-kappaB transcription and evasion of apoptosis," *J. Pharmacol. Exp. Therapeut.*, vol. 327, no. 3, pp. 746–759, Dec. 2008.

[99] C. Wilson, P. J. Maxwell, D. B. Longley, R. H. Wilson, P. G. Johnston, and D. J. Waugh, "Constitutive and treatment-induced CXCL8-signalling selectively modulates the efficacy of anti-metabolite therapeutics in metastatic prostate cancer," *PLoS ONE*, vol. 7, no. 5, 2012, Art. no. e36545.

[100] S. W. Ryter and A. M. Choi, "Targeting heme oxygenase-1 and carbon monoxide for therapeutic modulation of inflammation," *Transl. Res.*, vol. 167, no. 1, pp. 7–34, Jan. 2016.

[101] M. Walther *et al.*, "HMOX1 gene promoter alleles and high HO-1 levels are associated with severe malaria in Gambian children," *PLoS Pathog.*, vol. 8, no. 3, 2012, Art. no. e1002579.

[102] S. W. Ryter and R. M. Tyrrell, "The heme synthesis and degradation pathways: Role in oxidant sensitivity," *Free Radical Biol. Med.*, vol. 28, no. 2, pp. 289–309, 2000.

[103] D. M. Suttner and P. A. Dennery, "Reversal of HO-1 related cytoprotection with increased expression is due to reactive iron," *FASEB J.*, vol. 13, no. 13, pp. 1800–1809, Oct. 1999.

[104] N. F. Luz *et al.*, "Heme oxygenase-1 promotes the persistence of Leishmania chagasi infection," *J. Immunol.*, vol. 188, no. 9, pp. 4460–4467, May 2012.

[105] N. G. Abraham and A. Kappas, "Pharmacological and clinical aspects of heme oxygenase," *Pharmacol. Rev.*, vol. 60, no. 1, pp. 79–127, Mar. 2008.